Analysis of the Effects of Injecting Drug Use and HIV-1 Infection on ^{18}F-FDG PET Brain Metabolism

Michalis F. Georgiou[1], Ati Gonenc[1], Drenna Waldrop-Valverde[2], Russ A. Kuker[1], Shabbir H. Ezuddin[1], George N. Sfakianakis[1], and Mahendra Kumar[2]

[1]Department of Radiology, University of Miami School of Medicine, Miami, Florida; and [2]Department of Psychiatry and Behavioral Sciences, University of Miami School of Medicine, Miami, Florida

Injecting drug use (IDU) is a major risk factor for contracting HIV-1 infection. Both HIV and IDU are neurotoxic, and their coexistence may lead to increased dysfunction of brain metabolic processes. The objective of this research was to investigate the effects of HIV-1 infection and IDU on ^{18}F-FDG PET brain metabolism. **Methods:** ^{18}F-FDG PET brain imaging, with a standard clinical protocol, was performed on 59 subjects who belonged to 3 groups: HIV-positive/IDU-positive (n = 17), HIV-negative/IDU-positive (n = 13), and HIV-negative/IDU-negative controls (n = 29). A voxel-based analysis of the ^{18}F-FDG PET brain images was performed using statistical parametric mapping. The images were spatially normalized to a standard ^{18}F-FDG template, proportionally scaled to compensate for count differences, and then appropriately smoothed. Statistical 2-sample t tests were performed to determine regional metabolic distribution differences in the 3 groups. **Results:** Diffuse hypermetabolism in the subcortical and deep white matter, the basal ganglia, and the thalami was observed in HIV-1 infection. IDU resulted in increased brainstem metabolism and decreased activity in cortical structures including bilateral medial frontal lobes and the right inferior frontal and temporal cortices. The cortical hypometabolism was more extensive in HIV-1–infected subjects, involving the left temporoparietal and right parietal cortices and bilateral medial frontal lobes. **Conclusion:** Voxel-based analysis of ^{18}F-FDG PET brain images demonstrated statistically significant differences in regional metabolism for the 3 studied groups. It also showed that HIV-1 infection may have a synergistic effect with IDU, resulting in more extensive cortical hypometabolism. Correlation of these findings with other quantitative approaches and neurocognitive functioning is warranted.

Key Words: ^{18}F-FDG PET brain imaging; injecting drug use; HIV-1 infection; statistical parametric mapping

J Nucl Med 2008; 49:1999–2005
DOI: 10.2967/jnumed.108.052688

HIV remains a major health problem in the United States and abroad, with an estimated 40 million individuals infected worldwide (*1*). Significant progress has been made in the prevention and treatment of HIV-1 infection in recent years (*2*). Efforts are ongoing to learn more about the pathogenesis of the disease and, in particular, how it affects the central nervous system. ^{18}F-FDG PET has been used to evaluate the dynamic changes in regional cerebral metabolism associated with HIV-1 infection. Abnormal patterns of glucose metabolism in the brain have been reported for HIV-positive (HIV+) individuals, compared with HIV-negative (HIV−) healthy controls (*3–5*). Similarly, injecting drug use (IDU), which is considered to be a prominent risk factor for contracting and transmitting HIV-1 infection, has also been shown to affect regional brain metabolism, although the patterns of uptake may vary depending on the drug used (*6–8*).

Although the effects of HIV-1 infection and IDU on brain metabolism have been studied independently from each other, to our knowledge there has been no prior investigation of brain metabolism in HIV+ individuals (particularly those who are asymptomatic) who are also injecting drug users. Because both HIV and IDU can be neurotoxic, it has been hypothesized that their effects may be synergistic, leading to increased dysfunction of brain metabolic processes in those who are both HIV+ and injecting drug users.

The aim of this study was to investigate differences in cerebral glucose metabolism in HIV+ injecting drug users and HIV− injecting drug users, compared with control individuals. Because the effects of HIV and IDU on brain metabolism may be present long before neurologic symptoms are recognized, studying their combined influence could provide useful information in the management of the disease. A voxel-based analysis of the ^{18}F-FDG PET images was performed using statistical parametric mapping (SPM) (*9,10*) to evaluate changes in brain metabolism between the groups under investigation.

Received Apr. 1, 2008; revision accepted Aug. 11, 2008.
For correspondence or reprints contact: Michalis F. Georgiou, Nuclear Medicine (D-57), P.O. Box 016960, Miami, FL 33101.
E-mail: mgeorgio@med.miami.edu

MATERIALS AND METHODS

Study Participants

Participants in this study were part of a larger study investigating neuroendocrine changes associated with HIV-1 infection in injecting drug users. They were recruited from the streets and community of South Florida by trained outreach workers. A total of 59 participants, who belonged to the following 3 groups, were recruited for this study: group 1, HIV+/IDU-positive (IDU+) ($n = 17$); group 2, HIV−/IDU+ ($n = 13$); and group 3, HIV−/IDU-negative (IDU−), which was the control group ($n = 29$). All participants were between the ages of 20 and 45 y. The demographic information of the 3 groups is presented in Table 1. Injecting drug users (both HIV+ and HIV−) met diagnostic criteria for dependence on at least 1 substance. Control participants had no history of dependence on any substance. Serostatus of HIV+ participants was verified by examination of laboratory reports. HIV+ participants were free of any AIDS-defining symptoms at the time of the study. All participants were required to abstain from illicit drugs and alcohol for at least 12 h before the ^{18}F-FDG PET brain scan. Additionally, potential participants were excluded if they reported a history of loss of consciousness greater than 30 min, had a history of any neurologic surgery above the neck, or had a history of any neurologic disorder, including a history of central nervous system opportunistic infection for those with HIV-1 infection.

^{18}F-FDG PET

As part of this study, each participant received an ^{18}F-FDG PET scan in a relaxed resting state following a standard brain imaging protocol. The participants were instructed to have no caffeine or nicotine within 24 h before the scan, and they also had to fast overnight. On arrival at the hospital, they were asked to give a urine sample, which was tested for drug abstinence in compliance with the Triage 8 Panel for Drugs of Abuse (Biosite Inc.), which includes amphetamines, barbiturates, benzodiazepines, cannabinoids, cocaine, methadone, opiates, and PCP. The subjects were injected with ^{18}F-FDG (1.961 MBq/kg [0.053 mCi/kg]) after relaxing for 20 min in a darkened and quiet room. A resting period of 45 min followed, during which the subjects were comfortably seated with their eyes open, so they remained awake, and with outside stimuli kept to a minimum.

Imaging was performed for 40 min of acquisition time, using a C-PET Plus (Philips) dedicated ring detector scanner with a 2.54-cm (1-in)-thick sodium iodide crystal. The transverse and axial intrinsic spatial resolutions of the scanner are 5 and 5.5 mm in full width at half maximum (FWHM), respectively, at the center of the field of view. The images were attenuation-corrected using a 7-min transmission scan from a ^{137}Cs (740 MBq [20 mCi]) rotating point source. Images were reconstructed, using the manufacturer's software, with an ordered-subset expectation maximization algorithm (4 iterations, 8 subsets) into 128×128 matrices of isotropic voxels, with a slice thickness of 2 mm. The reconstructed transaxial slices were then realigned to yield sagittal and coronal images and also used to generate 3-dimensional volume-rendered images.

TABLE 1
Classification of Participants in Study

Parameter	Group 1: HIV+/IDU+	Group 2: HIV−/IDU+	Group 3 (Control): HIV−/IDU−
Number of patients (*n*)	17	13	29
Age (y)	40.3 ± 5.9	32.8 ± 7.7	31.6 ± 8.9
Sex (M/F)	13/4	10/3	16/13

Data are mean ± SD.

Image Preprocessing and SPM Analysis

Spatial preprocessing and statistical analysis were performed using SPM2 software (Wellcome Department of Cognitive Neurology, Institute of Neurology, University of College London) within MATLAB 7.0 (The MathWorks, Inc.) running on a Microsoft Windows XP machine.

The reconstructed image data were exported from the PET scanner in DICOM format and then converted using MRIcro software (developed by Chris Rorden; University of Nottingham Psychology, Nottingham, U.K.) into ANALYZE format, which is a supported input-data format for SPM2. The images were then transformed into a standard stereotactic space using affined and nonlinear transformations provided by SPM2 with the following default options: $7 \times 9 \times 7$ basis functions, 16 nonlinear iterations, and medium nonlinear regularization.

The template used for stereotactic normalization was an ^{18}F-FDG template specifically created for this study, rather than the standard SPM PET template, which was generated using ^{15}O-water (H_2O) PET images. The ^{18}F-FDG PET scans of 14 selected healthy subjects were first spatially normalized to the standard ^{15}O-H_2O PET template, and the ^{18}F-FDG PET template was built by averaging these normalized images and smoothing them by convolution with an isotropic gaussian kernel (8-mm FWHM).

The normalized scans (bounding box, −78:78, −112:76, −50:85; voxel sizes, $2 \times 2 \times 2$ mm; image size, $79 \times 95 \times 69$ mm; origin, (40, 57, 26)) were then smoothed with an isotropic gaussian kernel of 12-mm FWHM to increase the signal-to-noise ratio. To correct for intersubject variability in brain ^{18}F-FDG uptake due to differing amounts of injected ^{18}F-FDG dose and waiting periods from injection to scanning, the counts in each voxel were normalized to the global activity of each ^{18}F-FDG scan using the SPM technique of proportional scaling. The gray-level threshold was set to 0.8; that is, only voxels with intensities greater than 80% of the global normalized mean were included in the statistical analysis.

Two-sample *t* tests were used to detect differences between the HIV+/IDU+ (group 1) and the HIV−/IDU+ (group 2) groups and the control group (group 3). Brain areas with increased or decreased metabolic patterns in HIV+/IDU+ and HIV−/IDU+, compared with the controls, were calculated by using 2 different contrasts, [1 −1] and [−1 1], respectively. A *t* statistic for each voxel was subsequently generated, and the map SPM{T} was formed. The SPM{T} was then transformed to the unit normal distribution to give a gaussian field, or SPM{Z}, which was then thresholded at a probability level of P less than 0.005, uncorrected with the extent threshold for contiguous voxels set to $k = 100$.

The resulting areas that met the statistical criteria of significant difference were displayed as maximum-intensity projections (MIPs) collapsed onto a "glass-brain" representation in the 3

orthogonal planes. The obtained spatial coordinates were converted from Montreal Neurologic Institute (MNI) space to standard Talairach brain coordinates (*11*) using the Yale nonlinear Montreal Neurologic Institute to Talairach coordinate converter (*12*). The obtained converted coordinates were used to localize the brain regions in Talairach space using the Talairach Daemon (*13*).

RESULTS

SPM Analysis of HIV+/IDU+, Compared with HIV−/IDU− Controls

In the HIV+/IDU+ group, compared with the HIV−/IDU− control group, glucose metabolism was significantly reduced in the left temporoparietal cortex, left frontal subcortical white matter, medial frontal lobes, and right parietal cortex (Fig. 1A). Patterns with relative hypermetabolism were observed as diffuse activity in subcortical and deep white matter bilaterally, basal ganglia and thalami, medial temporal cortex, anterior cerebellum, and brainstem (Fig. 1B). Table 2 shows the comparison results of the most significant voxels and the corresponding Talairach coordinates.

SPM Analysis of HIV−/IDU+, Compared with HIV−/IDU− Controls

In the HIV−/IDU+ group, compared with the HIV−/IDU− controls, glucose metabolism was significantly reduced in the medial frontal lobes bilaterally and in the right inferior frontal and temporal cortices. Some relative hypometabolism was also noted in the right subcortical white matter (Fig. 2A). Relative hypermetabolism was seen in the medial parietal and occipital lobes, the brainstem, and the right occipital cortex (Fig. 2B). The most significant voxels and the corresponding Talairach coordinates are shown in Table 3.

SPM Analysis of HIV+/IDU+, Compared with HIV−/IDU+

In comparing the HIV+/IDU+ with HIV−/IDU+ group, we noted some relative hypometabolism in the left occipital lobe (Fig. 3A). Relative hypermetabolism was found as diffuse activity in subcortical and deep white matter bilaterally, basal ganglia and thalami, right medial frontal cortex, anterior cerebellum, and brainstem (Fig. 3B). Table 4 shows the comparison results of the most significant voxels and the corresponding Talairach coordinates.

DISCUSSION

Limited information has been published on the use of ^{18}F-FDG PET brain imaging to study the effects of HIV-1 infection and IDU on regional cerebral metabolic activity distribution. HIV seropositivity and IDU both affect cerebral glucose metabolism, and the effects may be present long before neurologic symptoms are recognized. Both HIV-1 infection and IDU have been shown to be neurotoxic, and in fact, it has been hypothesized that their effects may be synergistic, leading to increased dysfunction of brain metabolic processes in individuals who are both HIV+ and injecting drug users. To our knowledge, this study is unique in that it investigates the effects of HIV and IDU on ^{18}F-FDG PET brain metabolism and evaluates the potential synergistic interactions between them.

Our study demonstrated diffuse hypermetabolism in the subcortical and deep white matter, basal ganglia, and thalami that may be attributable to HIV-1 infection (observed in HIV+/IDU+ vs. HIV−/IDU− and HIV+/IDU+ vs. HIV−/IDU+, but not seen in HIV−/IDU+ vs. HIV−/IDU−). This hypermetabolic finding is consistent with published literature on brain metabolic distribution in HIV-1–infected individuals. In 1987, Rottenberg et al. (*3*) identified a pattern of relative regional hypermetabolism in patients with mild HIV-related dementia in subcortical regions (thalami and basal ganglia). This finding was confirmed in a study performed by van Gorp et al. (*14*) in 1992, comparing metabolic function and neuropsychologic status in patients with AIDS with HIV− controls. A significant increase in metabolism was revealed for the basal ganglia and thalami in subjects with AIDS without dementia when compared with the control group, suggesting early hypermetabolism in these subcortical structures. The study design excluded patients with a history of substance use or dependence (*14*). In 1996, Rottenberg et al. (*4*) further validated the earlier finding of subcortical hypermetabolism in a larger group of HIV-1–seropositive patients.

^{18}F-FDG PET in late-stage HIV-1 infection shows a somewhat different pattern of regional glucose distribution, with development of hypometabolism in both cortical and

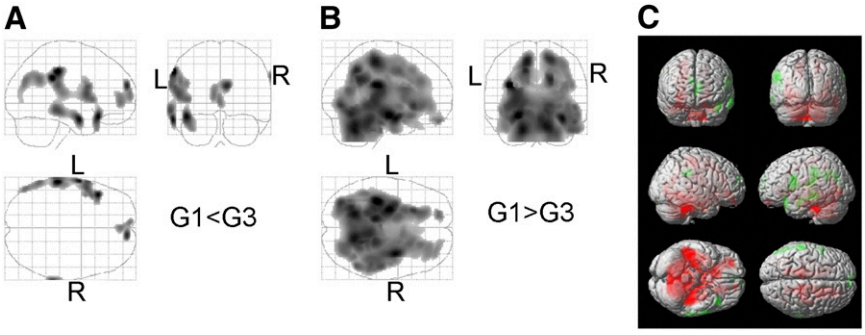

FIGURE 1. Two-dimensional MIP glass-brain representation showing areas of relative hypometabolism (A) and relative hypermetabolism (B) in HIV+/IDU+ group, compared with HIV−/IDU− controls. (C) Three-dimensional rendering of both hypermetabolism (red) and hypometabolism (green).

TABLE 2
SPM Significant Metabolic Differences Between HIV+/IDU+ Group and HIV−/IDU− Controls

Parameter	Cluster size (k voxels)	*z* score of maxima	Talairach coordinates* (mm)			Region
			x	*y*	*z*	
Relative hypometabolism	3,257	3.53	−59	−28	39	L, parietal lobe, postcentral gyrus
		3.48	−43	17	−13	L, temporal lobe, inferior frontal gyrus
		3.45	−59	−5	−16	L, temporal lobe, inferior temporal gyrus
	231	3.51	69	−35	33	R, parietal lobe, inferior parietal lobule
	663	3.36	9	57	19	R, frontal lobe, medial frontal gyrus
		3.07	0	46	−1	L, limbic lobe, anterior cingulate
		3.06	−8	59	7	L, frontal lobe, medial frontal gyrus
Relative hypermetabolism	65,099	4.94	−35	−27	24	L, parietal lobe, extranuclear
		4.90	−23	−12	−10	L, sublobar, extranuclear
		4.80	33	−4	21	R, sublobar, insula
	130	3.97	−16	48	−24	L, frontal lobe, superior frontal gyrus

*Coordinates corresponding to geographic center of cluster.
Height threshold $P < 0.005$, uncorrected for multiple comparisons. Extent threshold, k = 100 voxels.

subcortical areas not seen earlier in the disease process. Cortical and subcortical gray matter hypometabolism was reported by Rottenberg et al. (*3*) in patients with HIV who had more severe dementia. In 2000, Liow et al. (*15*) used voxel- and volume-of-interest–based quantitative techniques to analyze ^{18}F-FDG PET brain images of HIV-seropositive and HIV-seronegative healthy individuals. Their analysis identified areas of reduced glucose metabolism in the anterior frontal, occipital, and perisylvian cortices. Decreased glucose metabolism was also present in the parasagittal cortex abutting the anterior and posterior interhemispheric fissures and in the periventricular region.

In 1995, Depas et al. (*16*) reported cortical hypometabolism and subcortical hypermetabolism in children with severe neurologic symptoms who acquired HIV-1 infection perinatally. These children may represent an intermediate stage of the disease process in which cortical hypometabolism precedes subcortical hypometabolism. Therefore, it can be hypothesized that the subcortical hypermetabolism found in our study may reflect increased activity in HIV-infected neurons or may be a result of upregulation of proinflammatory cytokines (*17*). The resulting damage, whether direct or immune-mediated, leads to neuronal loss, causing increased hypometabolism over time and decreased activity reported in later stages of the disease. In addition, IDU may potentiate the relative hypermetabolic effects of early HIV infection on the white matter and deep gray structures, as evidenced by greater differences in the HIV+/IDU+ group versus the HIV−/IDU− controls than in the HIV+/IDU+ versus the HIV−/IDU+ groups.

In comparing the HIV−/IDU+ group with the HIV−/IDU− controls, we observed hypometabolism in the medial frontal cortex bilaterally, the right inferior frontal and temporal cortices, and the right temporal subcortical white matter. Cortical hypometabolism in substance abusers similar to that observed in our study has been reported in the literature. In 1988, using ^{15}O-H_2O PET, Volkow et al. (*6*) found that chronic cocaine users showed persistent decreases in relative cerebral blood flow in the prefrontal cortex when compared with healthy subjects. In 1992, Volkow et al. (*7*) used ^{18}F-FDG PET to demonstrate lower metabolic activity in frontal regions in neurologically intact chronic cocaine abusers, compared with controls, that persisted after months of detoxification. In 2005, Volkow et al. (*8*) demonstrated with ^{18}F-FDG PET the differing metabolic responses to intravenous methylphenidate in

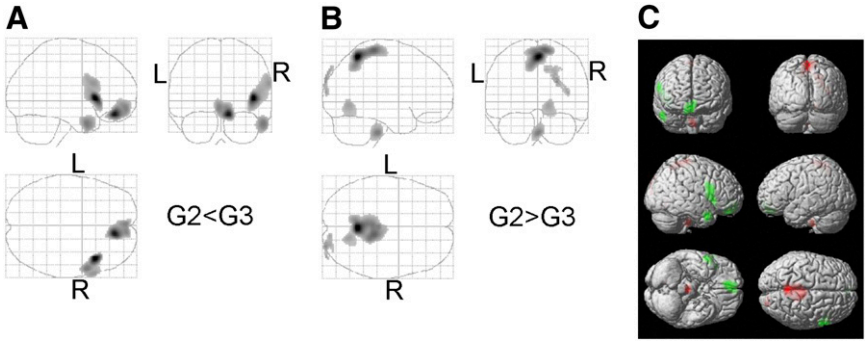

FIGURE 2. Two-dimensional MIP glass-brain representation showing areas of relative hypometabolism (A) and relative hypermetabolism (B) in HIV−/IDU+, compared with HIV−/IDU− controls. (C) Three-dimensional rendering of both hypermetabolism (red) and hypometabolism (green).

TABLE 3
SPM Significant Metabolic Differences Between HIV−/IDU+ Group and HIV−/IDU− Controls

Parameter	Cluster size (k voxels)	*z* score of maxima	Talairach coordinates* (mm)			Region
			x	*y*	*z*	
Relative hypometabolism	1,223	4.38	40	15	7	R, sublobar, insula
		3.16	61	13	23	R, frontal lobe, inferior frontal gyrus
	1,113	4.23	9	36	−17	R, frontal lobe, medial frontal gyrus
		2.39	−2	50	−11	L, frontal lobe, medial frontal gyrus
		2.27	7	52	−13	R, frontal lobe, medial frontal gyrus
	352	3.48	53	0	−22	R, temporal lobe, middle temporal gyrus
Relative hypermetabolism	1,991	4.42	2	−50	52	R, parietal lobe, precuneus
		3.72	10	−27	61	R, frontal lobe, subgyral
		3.55	−1	−30	59	L, frontal lobe, paracentral lobule
	111	3.31	26	−91	26	R, occipital lobe, cuneus
		3.07	41	−90	15	R, occipital lobe, middle occipital gyrus
		3.03	24	−87	34	R, occipital lobe, cuneus
	338	3.08	14	−63	0	R, occipital lobe, lingual gyrus

*Coordinates corresponding to geographic center of cluster.
Height threshold $P < 0.005$, uncorrected for multiple comparisons. Extent threshold, k = 100 voxels.

cocaine-addicted subjects and controls, with changes localized in the right medial orbital prefrontal cortex.

The effects of substance abuse on regional brain metabolism vary depending on the drug used. Although the IDU subjects in our study were primarily heroin and cocaine users, other drugs (e.g., marijuana, tobacco, or alcohol) may have been used that confound the metabolic effects shown by the performed analysis. Bolla et al. (*18*) in 2005, using ^{15}O-H_2O PET, demonstrated greater activation in the left cerebellum and less activation in the right lateral orbitofrontal cortex and dorsolateral prefrontal cortex of 25-d–abstinent heavy marijuana users, compared with the control group, during decision-making tasks. In 2004, Eldreth et al. (*19*) compared the performance on modified Stroop testing and ^{15}O-H_2O PET in 25-d–abstinent heavy marijuana users and controls. Although no significant deficits were detected in performance, marijuana users demonstrated hypoactivity in the left perigenual anterior cingulate cortex and lateral prefrontal cortex and hyperactivity in the hippocampus bilaterally. O'Leary et al. (*20*) in 2003 studied the effects of marijuana use on regional cerebral blood flow using ^{15}O-H_2O PET and found that smoking marijuana increased regional cerebral blood flow in the ventral forebrain and cerebellar cortex in both occasional and chronic users but resulted in significantly less frontal lobe activation in chronic users.

The present findings indicate that the cortical hypometabolism observed in our study comparing the HIV−/IDU+ group with HIV−/IDU− controls may reflect a direct action of the injected drug. Cortical hypometabolism was also seen in HIV+/IDU+ versus HIV−/IDU− but to a greater extent involving the left temporal-parietal cortex and right parietal cortex in addition to bilateral medial frontal lobes, which were also seen in HIV−/IDU+ versus HIV−/IDU−. Cortical hypoactivity has been reported in late-stage HIV-1 infection by many authors, as described above. That cortical hypometabolism was worse in the HIV+/IDU+ group than in the HIV−/IDU− controls may represent an indirect action of IDU accelerating the neurotoxic effects in HIV+ individuals who are also substance users. With the exception of minimally reduced activity in the left occipital lobe (present with $P < 0.005$

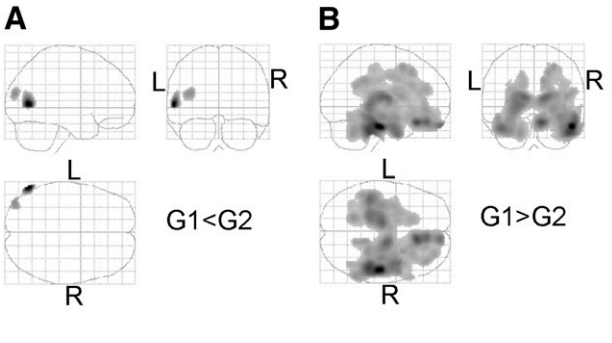

FIGURE 3. Two-dimensional MIP glass-brain representation showing areas of relative hypometabolism (A) and relative hypermetabolism (B) in HIV+/IDU+, compared with HIV−/IDU+. (C) Three-dimensional rendering of both hypermetabolism (red) and hypometabolism (green).

TABLE 4
SPM Significant Metabolic Differences Between HIV+/IDU+ and HIV−/IDU+ Groups

Parameter	Cluster size (k voxels)	*z* score of maxima	Talairach coordinates* (mm)			Region
			x	*y*	*z*	
Relative hypometabolism	255	3.53	−57	−67	8	L, temporal lobe, middle temporal gyrus
		2.92	−36	−83	19	L, occipital lobe, middle occipital gyrus
Relative hypermetabolism	32,933	5.21	47	−24	−20	R, temporal lobe, subgyral
		4.53	46	−36	−23	R, temporal lobe, fusiform gyrus
		4.53	9	23	−19	R, frontal lobe, rectal gyrus
	120	2.75	−13	−50	21	L, limbic lobe, limbic lobe, posterior cingulate

*Coordinates corresponding to geographic center of cluster.
Height threshold $P < 0.005$, uncorrected for multiple comparisons. Extent threshold, k = 100 voxels.

but not present when a more stringent criterion of $P < 0.001$ was used), no significant difference in hypometabolism between the HIV+/IDU+ and the HIV−/IDU+ groups was seen, suggesting that HIV-1 infection alone (in this group of early-stage HIV+ individuals) was not the principal cause of cortical hypometabolism.

In evaluating our findings, it is important to also address the limitations and methodologic issues of this study. All participants were free of opportunistic infection at the time of the study; however, viral load information for HIV+ subjects was not available, and thus the degree of disease progression could not be verified. In addition, insufficient information was available with respect to HIV+ subjects receiving highly active antiretroviral therapy (HAART), which may have introduced confounding effects on regional cerebral metabolism. Because injecting drug users in our region of South Florida commonly use many drugs, in addition to heroin and cocaine, our results likely reflect the summation of effects from multiple substances rather than from a single drug. Another limitation of the study is the relatively small sample sizes for the HIV+/IDU+ ($n = 17$) and HIV−/IDU− ($n = 13$) groups.

Future directions for this study include correlation of SPM findings with the outcomes of neurocognitive tests from the study participants. It would be interesting, for example, to correlate the more extensive left temporoparietal cortex hypometabolism noted in the HIV+/IDU+ versus the HIV−/IDU− controls, compared with the HIV−/IDU+ group versus the HIV−/IDU− controls, with functional deficiencies in language abilities or to correlate the observed reduction in metabolism in the medial frontal lobes with deficits in executive function. Confirmation of the SPM results with other quantitative techniques, such as standardized region-of-interest analysis, would be useful even though the superiority of SPM to such techniques has been well documented. A broader study design including PET/CT and functional MRI, with corresponding quantitative analysis from both modalities, may also provide useful insight as to the structural or anatomic changes that correlate with altered distribution in regional brain metabolism.

CONCLUSION

Voxel-based analysis of ^{18}F-FDG PET brain images using SPM demonstrated statistically significant differences in regional metabolism for the 3 studied groups: HIV+/IDU+, HIV−/IDU+, and HIV−/IDU− controls. It also showed that IDU may have a synergistic effect on HIV-1 infection, resulting in more extensive subcortical hypermetabolism and premature emergence of cortical hypometabolism. This synergism may have clinical implications, and ^{18}F-FDG PET can play a complementary role, along with other imaging modalities, in patient management. Correlation of our findings with other quantitative techniques and also neurocognitive analyses is warranted.

ACKNOWLEDGMENTS

We thank Peggy Gonzalez and Nisha Farrell for their help with this project. This research was supported by grant R01 DA 13550-SI awarded by the National Institute on Drug Abuse (NIDA), NIH.

REFERENCES

1. UNAIDS/WHO. AIDS Epidemic Update. UNAIDS/05.19E. December 2005. Available at: http://www.unaids.org/epi/2005/doc/EPIupdate2005_pdf_en/epi-update2005_en.pdf. Accessed September 25, 2008.
2. UNAIDS. Report on the Global AIDS Epidemic: Executive Summary. 06.20E. May 2006. Available at: http://data.unaids.org/pub/GlobalReport/2006/2006_GR-ExecutiveSummary_en.pdf. Accessed September 25, 2008.
3. Rottenberg DA, Moeller JR, Strother SC, et al. The metabolic pathology of the AIDS dementia complex. *Ann Neurol.* 1987;22:700–706.
4. Rottenberg DA, Sidtis JJ, Strother SC, et al. Abnormal cerebral glucose metabolism in HIV-1 seropositive subjects with and without dementia. *J Nucl Med.* 1996;37:1133–1141.
5. Pascal S, Resnick L, Barker WW, et al. Metabolic asymmetries in asymptomatic HIV-1 seropositive subjects: relationship to disease onset and MRI findings. *J Nucl Med.* 1991;32:1725–1729.
6. Volkow ND, Mullani N, Gould KL, Adler S, Krajewski K. Cerebral blood flow in chronic cocaine users: a study with positron emission tomography. *Br J Psychiatry.* 1988;152:641–648.
7. Volkow ND, Hitzeman R, Wang GJ, et al. Long-term frontal brain metabolic changes in cocaine abusers. *Synapse.* 1992;11:184–190.
8. Volkow ND, Wang GJ, Ma Y, et al. Activation of orbital and medial prefrontal cortex by methylphenidate in cocaine-addicted subjects but not in controls: relevance to addiction. *J Neurosci.* 2005;25:3932–3939.
9. Friston KJ, Frith CD, Liddle PF, Frackowiak RSJ. Comparing functional (PET) images: the assessment of significant change. *J Cereb Blood Flow Metab.* 1991;11:690–699.

10. Friston KJ, Holmes AP, Worsley KJ, Poline JB, Frith CD, Frackowiak RSJ. Statistical parametric maps in functional imaging: a general linear approach. *Hum Brain Mapp.* 1995;2:189–210.
11. Talairach J, Tournoux P. *Co-Planar Stereotaxic Atlas of the Human Brain.* New York, NY: Thieme Medical Publishers; 1988.
12. Nonlinear MNI to Talairach coordinate converter. Yale BioImage Suite Web site. Available at: www.bioimagesuite.org/Mni2Tal. Accessed September 25, 2008.
13. Lancaster JL, Woldorff MG, Parsons LM, et al. Automated Talairach atlas labels for functional brain mapping. *Hum Brain Mapp.* 2000;10:120–131.
14. van Gorp WG, Mandelkern MA, Gee M, et al. Cerebral metabolic dysfunction in AIDS: findings in a sample with and without dementia. *J Neuropsychiatry Clin Neurosci.* 1992;4:280–287.
15. Liow JS, Rehm K, Strother SC, et al. Comparison of voxel- and volume-of-interest-based analyses in FDG PET scans in HIV positive and healthy individuals. *J Nucl Med.* 2000;41:612–621.
16. Depas G, Chiron C, Tardieu M, et al. Functional brain imaging in HIV-1-infected children born to seropositive mothers. *J Nucl Med.* 1995;36:2169–2174.
17. Tucker KA, Roberston KR, Lin W, et al. Neuroimaging in human immunodeficiency virus infection. *J Neuroimmunol.* 2004;157:153–162.
18. Bolla KI, Eldreth DA, Matochik JA, Cadet JL. Neural substrates of faulty decision-making in abstinent marijuana users. *Neuroimage.* 2005;26:480–492.
19. Eldreth DA, Matochik JA, Cadet JL, Bolla KI. Abnormal brain activity in prefrontal brain regions in abstinent marijuana users. *Neuroimage.* 2004;23:914–920.
20. O'Leary DS, Block RI, Turner BM, et al. Marijuana alters the human cerebellar clock. *Neuroreport.* 2003;14:1145–1151.